JACC: CASE REPORTS VOL. 1, NO. 3, 2019

CASE REPORT

BEGINNER

CLINICAL CASE

Multimodality Imaging Reveals Divergent Responses of Left and Right Heart to Treatment in Cardiac Amyloidosis

Wolfgang Poller, MD,[a,b,*] Carsten Skurk, MD,[a,b,*] Felicitas Escher, MD,[b,c,d] Costantina Manes, MD,[a] Thomas Elgeti, MD,[e] Heinz-Peter Schultheiss, MD,[d] Matthias Taupitz, MD,[e] Ulf Landmesser, MD[a,b,f]

ABSTRACT

Cardiac amyloidosis is associated with very high morbidity and mortality. Only if treated early, cardiac amyloidosis responds well to therapy, and early recognition with a full differential diagnostic workup including multimodality imaging is therefore critical at first presentation. Closely meshed clinical monitoring and imaging are indispensable to ensure optimal individualized treatment. (**Level of Difficulty: Beginner.**) (J Am Coll Cardiol Case Rep 2019;1:360–6)

Amyloidosis encompasses a range of protein misfolding disorders causing organ dysfunction through fibril deposition (1). Cardiac involvement is associated with high mortality, and treatment options have been limited so far. The 2 main forms of cardiac amyloidosis (CA), light chain (CA_{AL}) and transthyretin (CA_{ATTR}) amyloidosis, have distinct pathomechanisms differentially addressed by pharmacotherapies (2). Regarding CA_{AL}, novel treatments beyond standard therapy with bortezomib are under investigation (3). Optimal monitoring of patients with CA_{AL} to enable early adaptation of therapy is dependent on diagnostic methods sensitive to key components (amyloid deposition, myocardial fibrosis, inflammation) of pathogenesis.

Noninvasive assessment of the response to therapy in CA_{AL} encompasses free light chains in serum and urine, N-terminal pro-B-type natriuretic peptide (NT-pro-BNP), echocardiography (4), and cardiac magnetic resonance (CMR) imaging (1). The authors previously found myocardial inflammation to indicate a significantly worse prognosis (5), a finding implying that detection of treatment effects on inflammation is desirable. The characterization of

LEARNING OBJECTIVES

- Only if treated early, CA_{AL} responds well to targeted therapies. Early recognition with a full differential diagnostic workup is indispensable at first presentation.
- Optimal individualized treatment requires close-meshed monitoring to enable early recognition of treatment failure, a prerequisite for therapeutic escalation before the "point-of-no-return" of right-sided heart failure.
- Multimodality imaging is essential for optimal pre-treatment risk stratification and assessment of differential treatment effects of novel therapeutics.

From the [a]Department of Cardiology, Campus Benjamin Franklin, Charite-Universitätsmedizin Berlin, Berlin, Germany; [b]German Center for Cardiovascular Research, Site Berlin, Berlin, Germany; [c]Department of Cardiology, Campus Virchow-Klinikum, Charite-Universitätsmedizin Berlin, Berlin, Germany; [d]Institute for Cardiac Diagnostics and Therapy, Berlin, Germany; [e]Institute for Radiology, Charite-Universitätsmedizin Berlin, Berlin, Germany; and the [f]Berlin Institute of Health, Berlin, Germany. *Drs. Poller and Skurk contributed equally to this work. The authors have reported that they have no relationships relevant to the contents of this paper to disclose.

Manuscript received May 13, 2019; revised manuscript received July 29, 2019, accepted July 31, 2019.

ISSN 2666-0849 https://doi.org/10.1016/j.jaccas.2019.07.034

myocardial inflammation requires both CMR (1) and endomyocardial biopsy (EMB) studies (6). The authors report on multimodality imaging revealing grossly divergent responses of the left and right sides of the heart to treatment in a patient with advanced CA_{AL}.

SEE PAGE 367

HISTORY OF PRESENTATION

A previously healthy 50-year-old woman presented with New York Heart Association functional class III to IV dyspnea that had insidiously developed over several months and had rapidly progressed within the last weeks. On first admission she was orthopneic and tachypneic, and auscultation revealed signs of pulmonary congestion.

PAST MEDICAL HISTORY

The patient had no past medical history except common childhood infectious diseases.

DIFFERENTIAL DIAGNOSIS

The differential diagnosis in this patient with the classical syndrome of heart failure with preserved ejection fraction (HFpEF) encompasses multiple types of cardiomyopathies, including genetic forms and storage diseases. To differentiate among these entities, additional laboratory, imaging (CMR, osteocomputed tomography), and biopsy (myocardium, bone marrow) studies, as well as molecular genetic mutation screening and amyloid subtyping in the EMBs, were conducted.

INVESTIGATIONS

Diagnostic studies included the following: *electrocardiography,* with nonspecific signs of disturbed repolarization and left ventricular (LV) hypertrophy (Supplemental Figure 1); *chest radiography,* with signs of chronic and acute pulmonary congestion (Supplemental Figure 1); *body plethysmography,* excluding pulmonary dysfunction; *echocardiography,* with concentric LV wall hypertrophy (15 mm), grade 3 diastolic dysfunction (E/A 3.0, E/E′ septal 29.2, lateral 24.5), "sparkling myocardium," and preserved LV ejection fraction (64%); and *CMR,* which yielded further functional and morphological information (**Figures 1A to 1D** and **2A to 2F**), as well as quantitative data on late gadolinium enhancement (LGE). The authors use phase-sensitive inversion recovery imaging because the image contrast of LGE versus normal myocardium is maximized over a wide range of inversion times. Phase-sensitive inversion recovery sequences are less prone to artifacts as a result of suboptimal myocardial nulling and are helpful if, as in this case, extensive LGE is present and the identification of normal myocardium is challenging.

Laboratory studies (**Figure 1A**), *CMR* (**Figures 1D** and **2B to 2F**), *EMB* (**Figures 1B, 1C,** and **2A**), and bone marrow biopsy identified cardiac involvement by CA_{AL}. Bone marrow showed plasma cells <10% of total, with no amyloid deposition. Cytometry identified 10% of all leukocytes as $CD45^{-}$ $CD38^{+}$ $CD138^{+}$ $CD56^{-}$ cells with light chain restriction λ. Cytogenetics identified no clonal structural or numerical chromosomal aberrations. No osseous destructions or anomalies appeared on a Paris protocol osteocomputed tomography scan. Serum creatinine was 0.69 mg/dl, glomerular filtration rate was >90 ml/min, hemoglobin was 13.7 g/dl, leukocytes were 10.4/nl, and thrombocytes were 176/nl. Immunofixation electrophoresis detected monoclonal free λ light chain excretion in the urine.

Mutation scanning of 173 cardiomyopathy-causing genes, performed because of sudden cardiac death in the patient's mother, detected a variant of unknown significance ($Gly^{193}Asp$) in the TBX20 gene but no known pathogenic defect, in particular not regarding hereditary amyloid-forming protein mutants or gene defects associated with hypertrophic or restrictive cardiomyopathies. Further, immunohistochemical amyloid subtyping in EMBs was negative for amyloid AA, ATTR AHγ, Aβ2M, atrial fibrillation, and AApoAI.

MANAGEMENT

In this patient, the diagnosis was established very late, with massive cardiac dysfunction at first presentation. The Mayo Clinic prognostic score, which is based on NT-pro-BNP, troponin, and free λ light chains, put her into stage III, with median survival ≈3 to 4 months. Detection of myocardial inflammation with massive perforin-positive cytotoxic T-cell infiltration (6) (**Figure 1B**) put her into a particularly high-risk group (5).

Reduction of the precursor protein that forms amyloid fibrils is prerequisite to improving prognosis in CA_{AL}. Treatment with bortezomib is considered standard in the treatment of CA_{AL}, for its tolerability and efficiency compared with chemotherapy. In addition, the patient was enrolled in a placebo-controlled phase 3 trial and was assigned to receive NEOD001 antibody-binding misfolded amyloid

ABBREVIATIONS AND ACRONYMS

AL = amyloid light chain

CA = cardiac amyloidosis

CMR = cardiac magnetic resonance

EMB = endomyocardial biopsy

LGE = late gadolinium enhancement

LV = left ventricular

NT-pro-BNP = N-terminal pro-B-type natriuretic peptide

FIGURE 1 Longitudinal Laboratory and Endomyocardial Biopsy Findings During Treatment

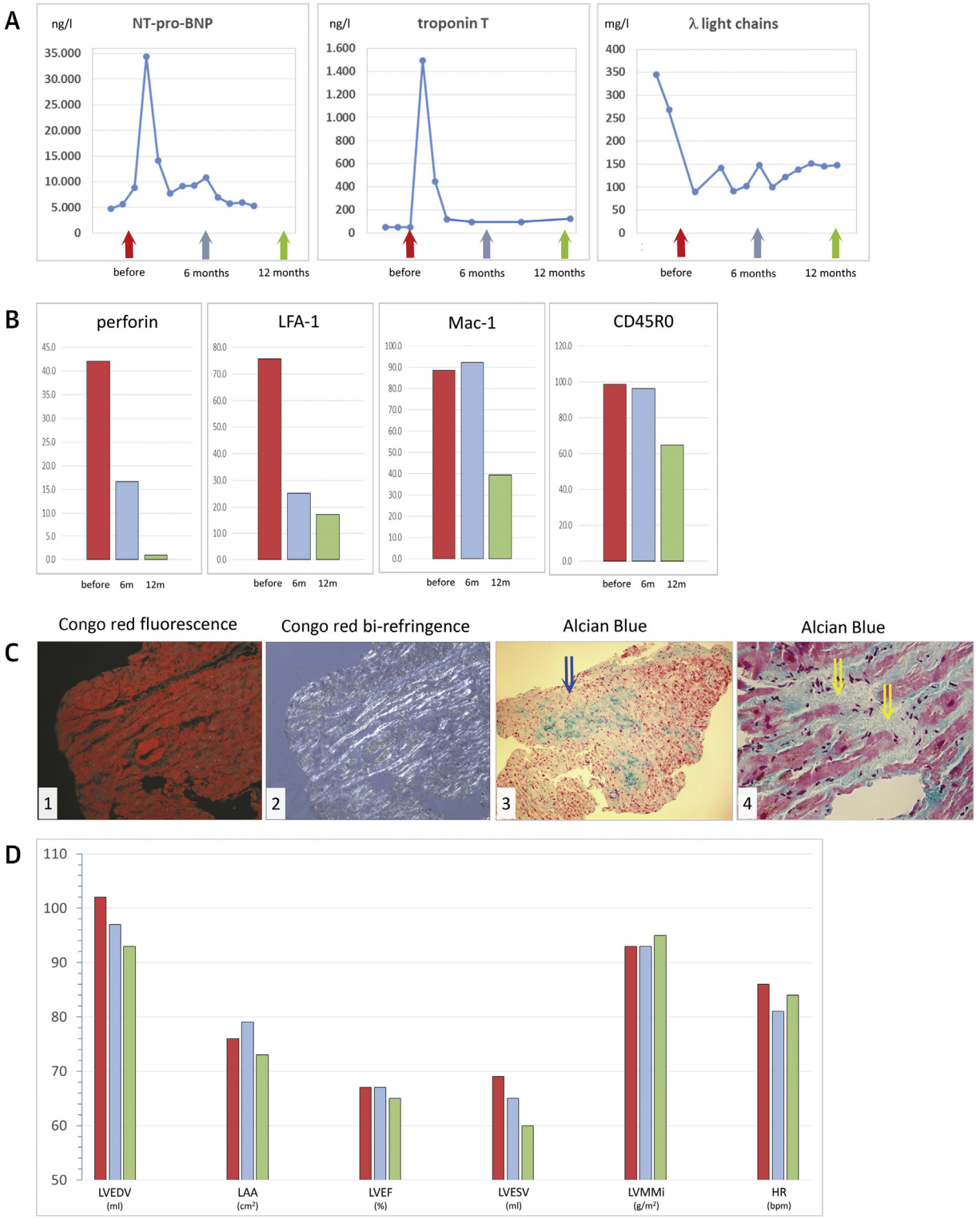

Continued on the next page

deposits (3). Sequential imaging including EMB enabled comparison of the systemic hematologic with local myocardial response, morphology, and function. Systemically, free λ light chains dropped from 344 mg/l (ratio κ/λ 0.04; Δ 330.4) to 90 mg/l (ratio κ/λ 0.12; Δ 79.8) and remained within this range for 12 months (**Figure 1A**). Locally in the myocardium, this was accompanied by highly significant regression of inflammation and disappearance of cytotoxic T cells (**Figure 1B**).

FOLLOW-UP

The clinical status of the patient rapidly improved from New York Heart Association functional class III to IV at initial presentation to class II 2 months after treatment initiation and remained stable for 12 months. In view of the expected survival of ≈3 of 4 months, this result implies therapeutic efficacy. However, stabilization was achieved for the left side of the heart only (**Figure 1D**). The concurrent development of insidiously progressive right-sided heart disease (**Figure 2**) was unexpected. After 15 months of therapy, free light chains rose rapidly to 224 mg/l (ratio κ/λ 0.1; Δ 201.5), and the patient died of refractory right-sided heart failure.

DISCUSSION

Patients presenting with advanced CA_{AL} and heart failure are an enormous clinical challenge. In these patients, high-dose therapy with melphalan has high treatment-related mortality and is commonly unfeasible (1). Our patient instead received standard therapy with the relatively well-tolerated proteasome inhibitor bortezomib in addition to NEOD001 antibody. Regarding inflammation, the decisive and enduring reduction of pre-treatment myocardial inflammation suggests that the local antiamyloid immune reaction responded well to this treatment. Regarding amyloid deposition, sequential EMBs showed transient regression of deposits after 6 months of treatment, possibly mediated by monocytes and macrophages infiltrating the myocardium. Consistent with the reduced inflammation and amyloid deposition, the treatment clearly stabilized the patient's left-sided heart disease. The observation of transient amyloid deposit regression is of interest in the context of pioneering experimental work attempting to induce immune cell-mediated degradation of amyloid deposits (7). Amyloid deposits appear to be at least partially reversible in humans, too, thus lending support to the respective approaches.

A critical clinical problem arises if light chains rise, myocardial inflammation is reignited, or cardiac function declines because no data from controlled clinical trials are available. Instead, an individualized response to each individual patient's problems is required. Systematic imaging of the treatment response in the patient highlights a hitherto neglected aspect of particular clinical interest. The authors describe grossly dichotomous development of left- and right-sided heart function and morphology. One possible explanation for this dichotomy is suggested by our observation (**Figure 2A**) that, in addition to amyloid disposal between cardiomyocytes, histologic examination also revealed pronounced amorphic amyloid material around microvessels, accompanied by perivascular inflammatory cells. This finding led to significant stenosis secondary to massive amyloid deposition and suggests amyloid-induced microvascular dysfunction as a pathomechanism not blocked by the treatment. In addition to perivascular amyloid, which we documented directly in the myocardium (**Figure 2A**), a published study proved that amyloid itself exerts adverse effects on vascular function (8). Amyloid deposits need not be confined to a single organ, and perivascular amyloid may therefore affect any vascular bed.

Because right ventricular dysfunction (4) is prognostically critical and a harbinger of terminal heart

FIGURE 1 Continued

(A) N-terminal pro-B-type natriuretic peptide (NT-pro-BNP), troponin T, free ʎ light chains *before* **(red arrows)** initiation of treatment with bortezumib (once weekly) plus NEOD001 (once monthly) and *after* 6 and 12 months **(blue and green arrows)**. There was a transient increase of initially only slightly elevated troponin T and NT-pro-BNP, whereas the clinical status of the patient continually improved. **(B)** Perforin-positive T cells, macrophage-1 antigen (Mac-1)–positive monocytes and macrophages, CD56RO-positive memory T cells, and vascular endothelial activation (lymphocyte function–associated antigen [LFA]-1) *before* treatment **(red bars)** and after 6 and 12 months **(blue and green bars)**. **(C) (1)** Congo red fluorescence showing amyloid (×400); **(2)** Congo red birefringence under polarized light amyloid (×400); **(3)** alcian blue stain of increased acidic mucopolysaccharides co-localized with amyloid **(arrow)**; **(4)** alcian blue–positive area with destruction of cardiomyocytes **(arrows)**. **(D)** Cardiac magnetic resonance showed stabilization of left ventricular function and morphology: left ventricular end-diastolic volume (LVEDV), left ventricular ejection fraction (LVEF), left ventricular myocardial mass index (LVMMi), and left atrial area (LAA). HR = heart rate; LVESV = left ventricular end-systolic volume.

FIGURE 2 **Cardiac Histology and Cardiac Magnetic Resonance Reveal Microvascular Disease and Progressive Right-Sided Heart Failure**

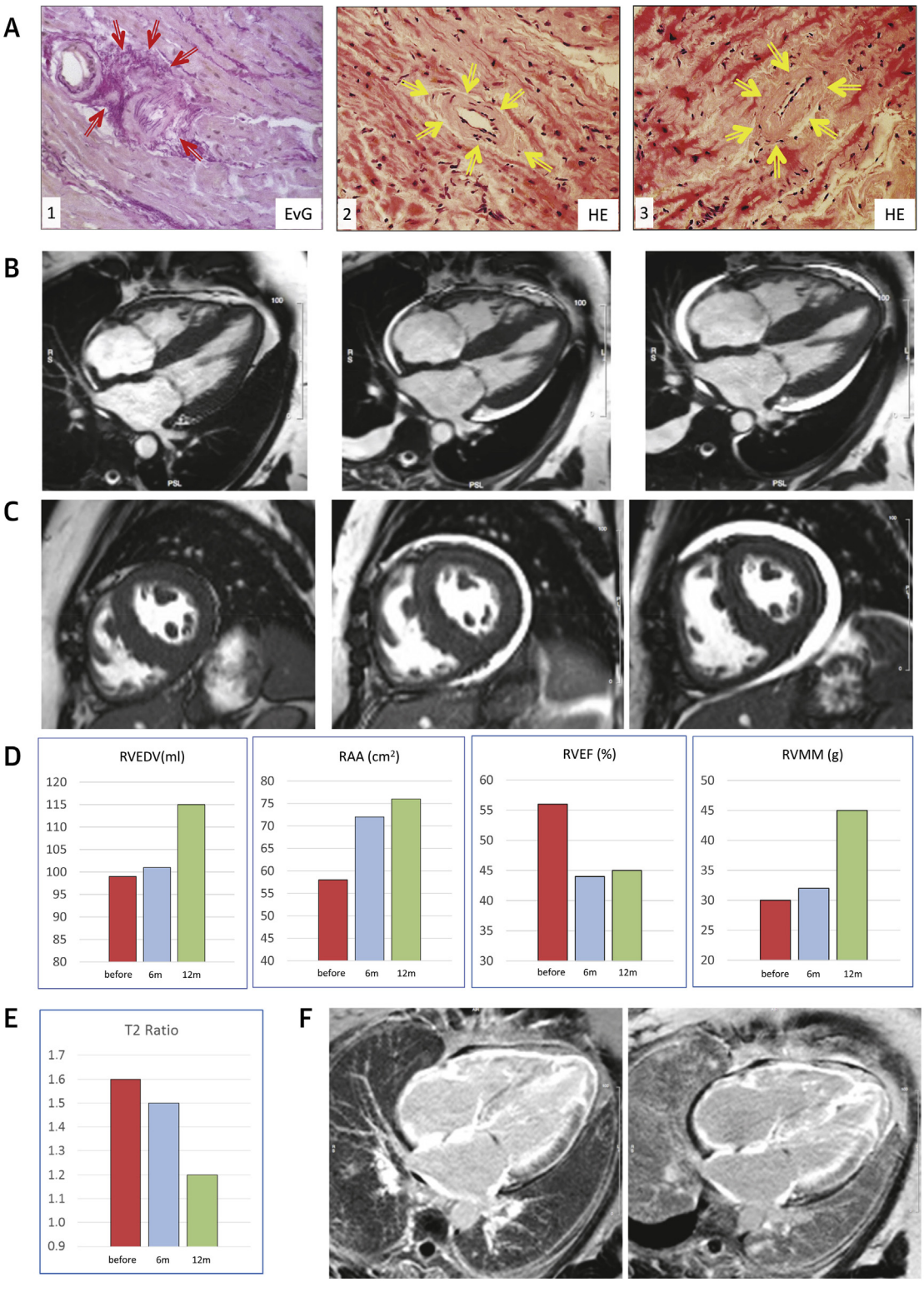

Continued on the next page

failure, possible amyloid-induced development of pulmonary vascular disease in CA_{AL} requires particular attention. Adequate treatment of pulmonary vascular disease needs detection in advance of an actual rise in pulmonary artery pressure, which occurs only late (9). The present case emphasizes that it is critical to pay close attention to the possible insidious development of right-sided heart failure even if, as in this patient, it is not apparent from a patient's good clinical status and standard laboratory and LV echocardiographic parameters. The authors therefore suggest invasive hemodynamic monitoring of patients with CA_{AL} as soon as right-sided heart function is impaired, to enable switching to more aggressive anti-plasma cell therapies *before* the "point of no return" of irreversible right-sided heart failure. Otherwise, progressive generalized whole body deposition of amyloid renders heart transplantation, which is a viable option for some patients, nonfeasible. Assist device implantation in CA_{AL} is problematic because of massive LV hypertrophy, in particular biventricular devices in the case of additional right-sided heart failure (10).

Regarding the development of novel therapeutics for patients with CA_{AL}, it is important to note that inclusion in the NEOD001 trial did *not* generally require histological documentation of myocardial amyloid deposits or characterization of the local immune response known to influence prognosis critically (5). The NEOD001 program was terminated because it was unable to detect clinical benefit of the antibody (VITAL Amyloidosis Study, a global phase 3, efficacy and safety study of NEOD001 in patients with AL amyloidosis [VITAL]; NCT02312206), thus leaving the challenge to proceed beyond stabilization to regression of organ involvement unsolved. From the current perspective, trial inclusion criteria (11) without multimodality imaging including EMB do not enable state-of-the-art prognostic risk stratification and, accordingly, subgroup analysis. More stringent inclusion criteria will be indispensable for future trials of novel therapeutics because they are prerequisites to elucidate the differential impact on the distinct pathomechanisms clinically relevant in CA_{AL}.

CONCLUSIONS

Optimal individualized treatment of patients with advanced CA_{AL} remains a major clinical challenge. One key point is the heterogeneity of these patients regarding their molecular pathomechanisms (e.g., amyloid deposition, inflammation). The importance of this is exemplified by the critical impact of myocardial inflammation on survival. Although it is impossible to deduce a general treatment strategy from published data, 2 conclusions are evident from the present case. First, each case requires optimal pre-treatment risk stratification. Second, invasive hemodynamic monitoring is indicated at the first signs of right ventricular dysfunction and/or pulmonary vascular disease. This will enable switching to more aggressive anti-plasma cell therapies *before* the "point of no return" of right ventricular failure and save the patient's option for heart transplantation.

ADDRESS FOR CORRESPONDENCE: Prof. Wolfgang Poller, Department of Cardiology, Campus Benjamin Franklin, Charite Centrum 11, Charité-Universitätsmedizin Berlin, Hindenburgdamm 30, 12200 Berlin, Germany. E-mail: wolfgang.poller@charite.de.

FIGURE 2 Continued

(A) In addition to the well-known disposal of amyloid among cardiomyocytes (Figure 1D), in this patient with massive myocardial inflammation (Figure 1C), Elastica van Gieson (EvG) and hematoxylin and eosin (HE) staining revealed pronounced amorphic amyloid material **(yellow arrows)** and inflammatory cells **(red arrows)** surrounding vessels with thickened wall and stenosis secondary to massive amyloid deposits **(arrows)**. **(B)** Longitudinal cardiac magnetic resonance studies (4-chamber-view) *before* treatment **(left)** and *after* 6 or 12 months **(middle or right)** (cine steady-state free-precession imaging). Although the left chambers remained constant, the right ventricle and right atrium progressively dilated. **(C)** Short-axis views analogous to those in **B. (D)** Development of right-sided heart functional and morphological parameters: right ventricular end-diastolic volume (RVEDV), right ventricular ejection fraction (RVEF), right ventricular myocardial mass (RVMM), and right atrial area (RAA). In contrast to the patient's stable left-sided heart status (Figure 1D), there was massive dilation of the right heart chambers, a decline of contractile function (right ventricular ejection fraction), and increased right ventricular mass by 50% compared with baseline. **(E)** The T2 ratio remained stable initially and then rapidly declined between 6 and 12 months of therapy. **(F)** Late gadolinium enhancement imaging using phase-sensitive inversion-recovery imaging at baseline **(left)** and follow-up **(right)** displays enhancement in the atrial walls, the right ventricular free wall, diffuse enhancement of the septum, and more subendocardial distribution of the left ventricular free wall.

REFERENCES

1. Maurer MS, Elliott P, Comenzo R, Semigran M, Rapezzi C. Addressing common questions encountered in the diagnosis and management of cardiac amyloidosis. Circulation 2017;135:1357–77.

2. Poller W, Dimmeler S, Heymans S, et al. Non-coding RNAs in cardiovascular diseases: diagnostic and therapeutic perspectives. Eur Heart J 2018;39:2704–16.

3. Gertz MA, Landau H, Comenzo RL, et al. First-in-human phase I/II study of NEOD001 in patients with light chain amyloidosis and persistent organ dysfunction. J Clin Oncol 2016;34:1097–103.

4. Bodez D, Ternacle J, Guellich A, et al. Prognostic value of right ventricular systolic function in cardiac amyloidosis. Amyloid 2016;23:158–67.

5. Siegismund CS, Escher F, Lassner D, et al. Intramyocardial inflammation predicts adverse outcome in patients with cardiac AL amyloidosis. Eur J Heart Fail 2018;20:751–7.

6. Escher F, Kühl U, Lassner D, et al. High perforin-positive cardiac cell infiltration and male sex predict adverse long-term mortality in patients with inflammatory cardiomyopathy. J Am Heart Assoc 2017;6:e005352.

7. Richards DB, Cookson LM, Berges AC, et al. Therapeutic clearance of amyloid by antibodies to serum amyloid P component. N Engl J Med 2015;373:1106–14.

8. Franco DA, Truran S, Weissig V, et al. Monosialoganglioside-containing nanoliposomes restore endothelial function impaired by AL amyloidosis light chain proteins. J Am Heart Assoc 2016;5:e003318.

9. Lau EM, Manes A, Celermajer DS, Galie N. Early detection of pulmonary vascular disease in pulmonary arterial hypertension: time to move forward. Eur Heart J 2011;32:2489–98.

10. Mehra MR, Canter CE, Hannan MM, et al. The 2016 International Society for Heart Lung Transplantation listing criteria for heart transplantation: a 10-year update. J Heart Lung Transplant 2016;35:1–23.

11. Liedtke M, Merlini G, Landau H, et al. The VITAL amyloidosis study: a Randomized, double-blind, placebo-controlled, global, phase 3 study of NEOD001 in patients with AL amyloidosis and cardiac dysfunction. Blood 2016;128:5690.

KEY WORDS cardiac amyloidosis, cardiomyopathies, cardiovascular inflammation, endomyocardial biopsy, immunosuppressive therapy, myocardial imaging

APPENDIX For a supplemental figure, please see the online version of this paper.